phys. stat. sol. (b) **202**, 247 (1997)

Subject classification: 68.55.Jk; 68.55.Ln; S6

Step-Controlled Epitaxial Growth of High-Quality SiC Layers

T. KIMOTO, A. ITOH, and H. MATSUNAMI

Department of Electronic Science and Engineering, Kyoto University, Yoshidahonmachi, Sakyo, Kyoto 606-01, Japan

(Received January 31, 1997)

The growth mechanism in chemical vapor deposition (CVD) of silicon carbide (SiC) on off-oriented SiC{0001} substrates (step-controlled epitaxy) is reviewed. In step-controlled epitaxy, SiC growth is controlled by the diffusion of reactants in a stagnant layer. Critical growth conditions where the growth mode changes from step-flow to two-dimensional nucleation are predicted as a function of growth conditions using a model describing SiC growth on vicinal {0001} substrates. Step bunching on the surfaces of SiC epilayers is also investigated. Dominant step heights correspond to the half or full unit cell of SiC polytypes. The high quality of the SiC epilayers has been elucidated through Hall effect and deep level measurements. Excellent doping controllability in a wide range has been obtained by in-situ doping of a nitrogen donor and an aluminum acceptor.

1. Introduction

Silicon carbide (SiC) has received increasing attention as a wide bandgap semiconductor material for high-power, high-frequency, high-temperature and radiation-resistant devices. In particular, theoretical simulation has predicted that SiC power switching devices can replace the present-day Si power devices on account of much lower dissipation and reduced chip sizes [1].

Although chemical vapor deposition (CVD) has advantages in the precise control and uniformity of epilayer thickness and impurity doping, there had been a serious problem of polytype mixing in CVD growth of α-SiC [2 to 4]. In 1986 to 1987, the authors' group found that single crystalline 6H-SiC can be homoepitaxially grown on off-oriented 6H-SiC{0001} at low temperatures of 1400 to 1500 °C [5, 6]. Independently, Kong et al. [7] also succeeded in homoepitaxial growth of 6H-SiC using off-oriented substrates. This technique was named *"step-controlled epitaxy"*, since the polytype of epilayers can be controlled by surface steps existing on the off-oriented substrates. This technique was an epoch-making breakthrough in two senses that (i) growth temperature can be reduced more than 300 °C and (ii) epilayers have very high quality enough for device applications. Today, device-quality α-SiC epilayers have been produced by this technique through the world [8 to 13], supporting recent progress of SiC device fabrication [14].

In this paper, the mechanism of step-controlled epitaxial growth of SiC is reviewed. High-quality of SiC epilayers is presented through optical and electrical characterization.

2. Experiments

Fig. 1 shows a schematic diagram of the CVD growth system used at the authors' group. Crystal growth was carried out by atmospheric pressure CVD in a horizontal reaction tube. SiH_4 (1% in H_2) and C_3H_8 (1% in H_2) were used as source gases. The carrier gas was H_2 purified with an Ag–Pd purifier. The flow rates of SiH_4 and C_3H_8 were 0.10 to 0.60 sccm (typically 0.30 sccm) and 0.10 to 0.80 sccm (typically 0.20 sccm), respectively. The H_2 flow rate was fixed at 3.0 slm, which provides a linear gas velocity of 6 to 10 cm/s above the substrates. N_2 was used for n-type doping, and trimethylaluminum ($TMA : Al(CH_3)_3$) and B_2H_6 for p-type doping. Hydrogen chloride (HCl) gas was used for etching of a substrate surface before CVD growth.

Two kinds of α-SiC crystals were used as substrates, crystals grown by the Acheson method or a modified Lely (sublimation) method. Since the basal plane of the Acheson crystals is {0001} face, the off-oriented substrates were prepared by angle-lapping of the basal plane. As for crystals grown by a modified Lely method, both commercially available and homemade wafers were used. The substrate off-angle was 0 to 10° (typically 5 to 6°) toward $\langle 11\bar{2}0 \rangle$. SiC{0001} is a polar face, being either (0001) Si or (0001) C. Both Si and C faces were used to investigate the substrate polarity effects. The polarity was identified by thermal oxidation at 1000 °C for 5 h utilizing the difference in oxidation rates between both faces (oxidation is faster on $(000\bar{1})$ C faces) [15, 16]. The polytypes of substrates were identified by the absorption edges in ultraviolet-visible light transmission spectra and photoluminescence, and were confirmed by X-ray diffraction and Raman scattering.

Substrates were set on a SiC-coated graphite susceptor, and heated by radio frequency (rf) induction. Before the CVD growth, in-situ HCl etching was performed to remove surface damage introduced by the polishing process. The growth temperature was varied in the range of 1100 to 1600 °C (typically 1500 °C).

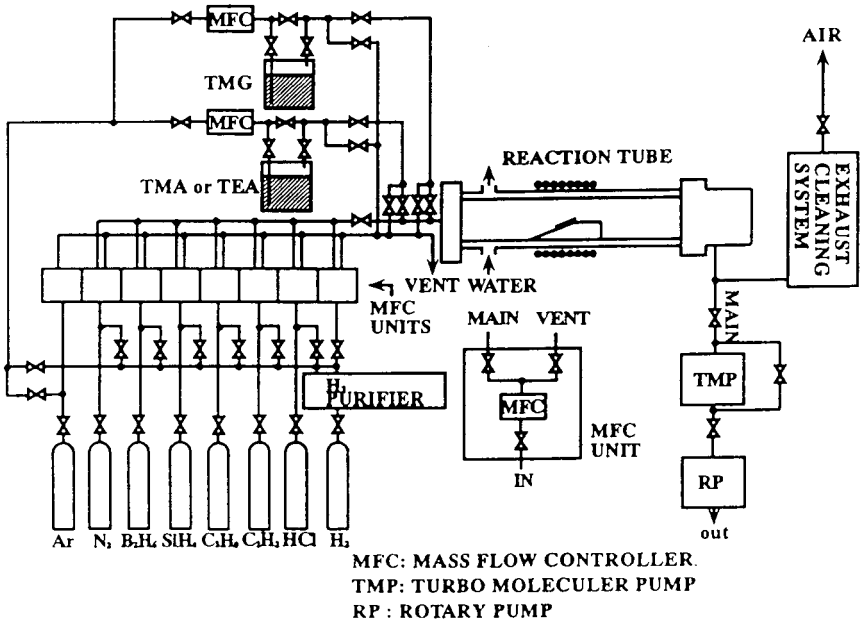

Fig. 1. Schematic diagram of the CVD system used in the authors' group

3. Epitaxial Growth

3.1 Growth mode

Fig. 2 shows Nomarski microphotographs of 5 μm thick SiC layers grown on a) well-oriented and b) 6° off-oriented 6H-SiC(0001) substrates at 1500 °C under a typical gas flow condition (SiH_4: 0.30 sccm, C_3H_8: 0.20 sccm). On a well-oriented (0001) face, the epilayer shows a mosaic pattern, and smooth domains are separated by step- or groove-like boundaries. From the reflection high-energy electron diffraction (RHEED) analysis, the grown layer was identified as 3C-SiC(111) with double positioning twinning [17]. On a well-oriented $(000\bar{1})$ C face, the grown surface is rough, and island-like growth is observed (not shown). The RHEED analysis revealed that the grown layer is also twinned crystalline 3C-SiC.

In contrast, epilayers on off-oriented substrates exhibit specular, smooth surfaces. The grown layer was identified as 6H-SiC(0001) by RHEED and transmission electron microscope (TEM) observation. Homoepitaxial growth with excellent surface morphology can also be achieved on an off-oriented $(000\bar{1})$ C face. Surface morphology depends on growth rate and especially temperature, of which details are discussed later.

On well-oriented {0001} faces, the step density is very low and vast terraces exist. Then, crystal growth may initially occur on terraces through two-dimensional nucleation due to the high supersaturation on the surface. The polytype of grown layers is determined by growth conditions, mainly growth temperature. This leads to the growth of 3C-SiC, which is stable at low temperatures. This phenomenon has been predicted by theoretical studies using a quantum-mechanical energy calculation [18] and an electrostatic model [19]. As the stacking order of 6H-SiC is ABCACB ... in the ABC notation [20], the growing 3C-SiC can take two possible stacking orders of ABCABC ... and ACBACB ..., as shown in Fig. 3a, leading to double positioning twins. On off-oriented substrates, the step density is high, and the terrace width is narrow enough for adsorbed species to reach steps. At a step, the incorporation site is uniquely determined by bonds from the step, as shown in Fig. 3b. Hence,

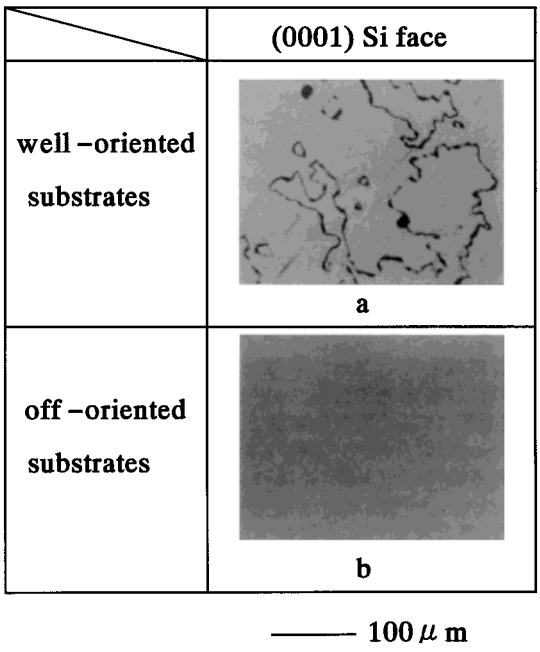

Fig. 2. Surface morphology of SiC layers grown on a) well-oriented and b) 6° off-oriented 6H-SiC(0001) Si substrates. Growth temperature and growth rate are 1500 °C and about 2 μm/h, respectively

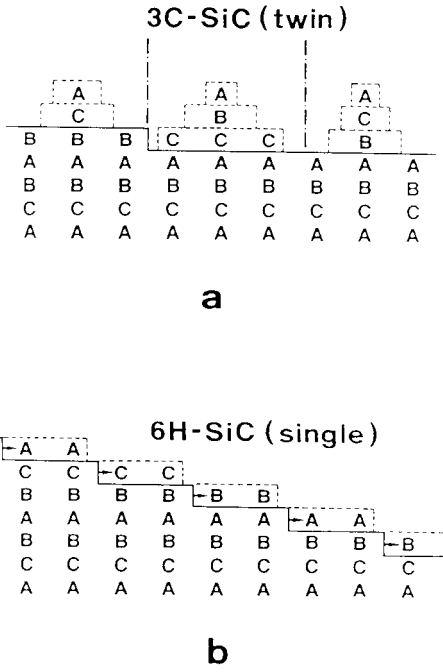

Fig. 3. Schematic images of the relationship between growth modes and polytypes of layers grown on 6H-SiC{0001}. a) 3C-SiC is grown through two-dimensional nucleation, and b) homoepitaxy of 6H-SiC is achieved owing to step-flow growth

homoepitaxy can be achieved through the lateral growth from steps (step-flow growth), inheriting the stacking order of substrates, i.e. surface steps serve as a template which forces the replication of the substrate polytype in the epilayer. This growth technique is applicable to homoepitaxy of any other polytypes such as 4H-SiC [21], 15R-SiC, and 21R-SiC [22]. Tairov et al. [23] investigated the effects of substrate off-angle in epitaxial growth of SiC at 1600 to 2200 °C by a sandwich growth method. They observed the stable homoepitaxy without 3C-SiC inclusions on off-oriented substrates.

The cause of 3C-SiC nucleation on off-oriented substrates has been investigated by Powell et al. [24]. They have investigated the effcts of off-angle and surface treatment on the polytypes of grown layers, and found that homoepitaxy of 6H-SiC is possible even on substrates with a low-tilt angle of 0.2° and 3C-SiC nucleation takes place at defect sites on the surface. The defects can be screw dislocations or surface damages introduced by polishing. More recently, Hallin et al. [25] reported that substrate imperfection and surface defects induce the development of large (0001) facets on which 3C-SiC inclusions are created via spontaneous nucleation, which is much more pronounced in 4H-SiC growth than 6H-SiC. All these facts indicate that it is essential to keep supersaturation low enough to ensure "perfect step-flow growth", thus enabling homoepitaxy of α-SiC. The improvement of 6H-SiC epilayer quality by utilizing off-oriented substrates has also been reported in LPE [26]. Thus, the use of off-oriented substrates may be a key technique in various SiC growth methods.

The off-direction dependence in CVD growth of 6H-SiC has been reported by Kong et al. [7] and Ueda et al. [27]. On a 6H-SiC(0001) Si face inclined toward $\langle 1\bar{1}00\rangle$, stripe-like morphology, which is caused by pronounced step bunching, appeared and the inclusion of 3C-SiC domains was observed by long-time growth. Based on these results, the off-direction toward $\langle 11\bar{2}0\rangle$ has mainly been employed in almost all the groups.

3.2 Growth mechanism

At a C/Si ratio (the ratio between the number of C and Si atoms in supplied gases) greater than 1.4, where good morphology without Si droplets can be obtained in the present growth system, the growth rate increases proportionally with the flow rate of SiH_4, indicating that Si species limit SiC growth. Karmann et al. [28] also investigated the growth on off-oriented 6H-SiC(0001) faces using SiH_4 and C_3H_8 at 1500 to 1600 °C, and observed that the supply of SiH_4 controlled the rate of SiC growth.

Allendorf and Kee [29] have analyzed gas-phase and surface reactions at 1200 to 1600 °C in a SiH_4–C_3H_8–H_2 system. Stinespring and Wohmhoudt [30] also reported a similar analysis on gas-phase kinetics. Their analyses have shown that the dominant species which contribute to SiC growth may be Si, SiH_2, Si_2H_2 species from SiH_4, and CH_4, C_2H_2, C_2H_4 molecules from C_3H_8. This simulation suggests that Si (or SiH_2) may be preferentially adsorbed and migrate on the surface. In fact, almost no deposition occurs in the present CVD system without SiH_4 supply. Recently, the effective C/Si ratio in vapor in the vicinity of a substrate surface has been estimated to be about 100 or higher at an "input" C/Si ratio of 2 [31]. This fact means that growth environment is extremely C-rich, making the supply of Si species be a major limiting factor of growth rate.

The authors systematically investigated the effects of C/Si ratio on surface morphology. At 1500 °C, epilayers on Si faces showed specular, smooth surfaces for the C/Si ratios between 2 and 6. On C faces, the optimum C/Si ratio window is relatively narrow, from 2 to 3. This tendency is independent of substrate polytypes, 6H or 4H. However, epitaxial growth 4H-SiC on Si faces is very sensitive to polishing damage and/or substrate defects. Triangular pits and macrosteps are easily formed at the defect sites. A recent work revealed that 3C-SiC nucleation takes place on most triangular pits (triangular stacking faults) [25]. Though the appearance of these surface defects can be suppressed by reducing surface damage and improving CVD procedures [32], it is noteworthy that these defects appear only on Si faces. Epilayer surfaces on C faces are very flat even for 4H-SiC as far as the C/Si ratio is in the range from 2 to 3.

Fig. 4 shows the growth rates for various off-angles of the substrate at 1500 °C [33]. The flow rates of SiH_4 and C_3H_8 are 0.30 and 0.20 sccm, respectively. In this figure, open (on a Si face) and closed (on a C face) triangles mean the growth of 3C-SiC, and open and closed circles mean that of 6H-SiC. 6H-SiC can be homoepitaxially grown on off-oriented substrates with more than 1°. On well-oriented substrates (off-

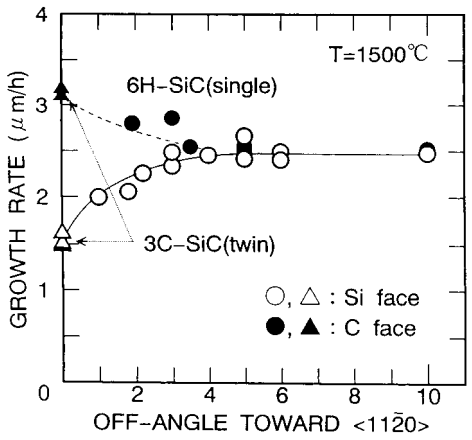

Fig. 4. Dependence of growth rate at 1500 °C on off-angle of the substrate. The flow rates of SiH_4 and C_3H_8 are 0.30 and 0.20 sccm, respectively. Open and closed triangles show growth of 3C-SiC, and circles denote that of 6H-SiC

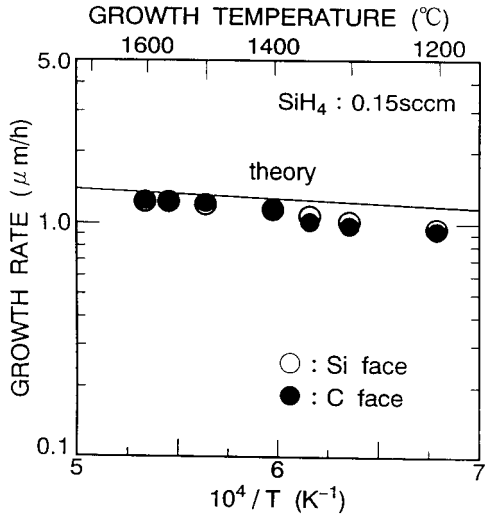

Fig. 5. Temperature dependence of growth rate on 6° off-oriented 6H-SiC(0001) Si and (000$\bar{1}$) C faces. The flow rates of SiH_4 and C_3H_8 are 0.15 and 0.10 to 0.14 sccm, respectively. The calculated result based on a stagnant layer model is shown by a solid curve

angle = 0°) higher growth rates are obtained on C faces, as has been reported [34]. This might be ascribed to the higher nucleation rate on (000$\bar{1}$) C terraces [35]. With increasing off-angle, the growth rates on both faces approach each other and become almost the same value of 2.5 μm/h for off-angles from 4° to 10°.

Fig. 5 shows the temperature dependence of the growth rate in the range between 1200 and 1600 °C, in which homoepitaxial growth of 6H-SiC occurs [33, 36]. The flow rates of SiH_4 and C_3H_8 are 0.15 and 0.10 to 0.14 sccm, respectively, and the off-angle is 5 to 6°. The temperature dependence of the growth rate yields a very small activation energy of 12 kJ/mol. For CVD growth on well-oriented {0001} faces, activation energies of 50 [34], 84 [37] or 92 kJ/mol [2] were reported. There is little difference between the growth rates on Si and C faces even at low temperatures. Karmann et al. [28] also reported similar insensitivity of growth rate to temperature in CVD on 6H-SiC substrates with a 2° off-angle toward ⟨1$\bar{1}$00⟩.

The solid curve in Fig. 5 denotes the theoretical growth rate calculated with a stagnant layer model, which has been developed in Si CVD [38]. The absolute values of growth rate calculated from the simple model show surprisingly good agreement with

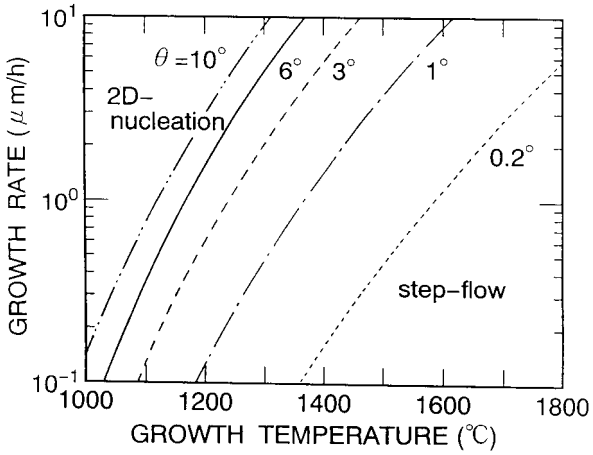

Fig. 6. Critical growth conditions as a function of growth temperature, growth rate, and off-angles of the substrate ($\theta = 0.2°$, 1°, 3°, 6°, and 10°). The top-left and bottom-right regions from the curves correspond to two-dimensional nucleation and step-flow growth conditions, respectively

experimental values. The predicted growth rate increases gradually with temperature increase, owing to the enhancement of diffusion in a stagnant layer. The calculated curve in the range of 1200 to 1600 °C yields an apparent activation energy of 10 kJ/mol using the method of least squares, in very good agreement with the experimental result. Therefore, the growth would be limited by mass transport in step-controlled epitaxy. This fact gives good explanation for little difference in the growth rates on Si and C faces, because no polarity dependence should be observed in the growth controlled by mass transport.

The "step-flow growth window", where homoepitaxy of SiC is realized through step-flow is of great interest. For example, the authors found that 6H-SiC can be homoepitaxially grown on a 6° off-oriented substrate at 1200 °C, but not at 1100 °C [33]. Using a simple surface diffusion model based on the BCF (Burton, Cabrera, and Frank) theory [39] and some experimental data, we determined the critical growth conditions where growth mode changes from step-flow (6H- or 4H-SiC growth) to two-dimensional nucleation (3C-SiC growth) [40]. Critical growth conditions are shown by the curves in Fig. 6 for substrate off-angles of 0.2°, 1°, 3°, 6°, and 10°. In the figure, the top-left and bottom-right regions separated by the curves correspond to the two-dimensional nucleation and step-flow growth conditions, respectively. Almost no difference in the critical conditions was obtained on Si and C faces. The higher growth rate and lower off-angle are available for step-flow growth at higher growth temperatures. At 1800 °C, a very small off-angle of 0.2°, which yields almost "well-oriented" faces, is enough to achieve step-flow growth with a moderate growth rate of 6 μm/h. This may be one of the reasons why 6H-SiC can be homoepitaxially grown on well-oriented faces if the growth temperature is raised up to 1700 to 1800 °C [2 to 4]. The role of defects for 3C-SiC nucleation may become important on substrates with small off-angles [24]. On the contrary, large off-angles more than 5° are needed to realize homoepitaxy of 6H-SiC at a low temperature of 1200 °C with a growth rate of 1 μm/h.

3.3 Step bunching

In SiC growth, quite a few studies have been reported about step structure on high-quality CVD-grown α-SiC surfaces [41 to 44]. In the present study, as-grown samples without any surface treatments were examined using atomic force microscopy (AFM) and TEM observations. Fig. 7a, b show the height profiles of 6H-SiC epilayers grown on (0001) Si

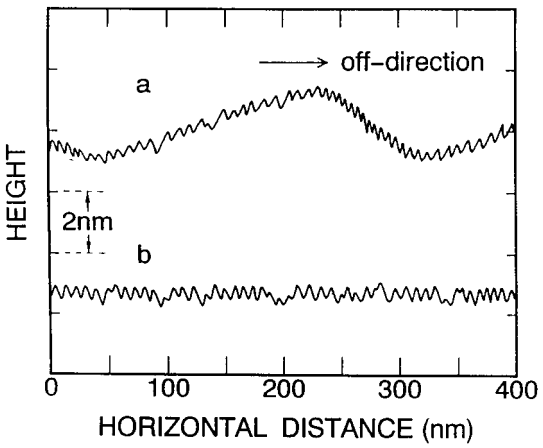

Fig. 7. Height profiles of 6H-SiC epilayers grown on 5° off-oriented (a) 6H-SiC(0001) Si and (b) (000$\bar{1}$) C faces. The surface steps go down from the left to the right

and $(000\bar{1})$ C faces, respectively, obtained from AFM data [42]. The off-angle of the substrates is 5°, and the steps go down from the left to the right. A distinctive difference in the surface structure between both the faces can be observed. Epitaxial growth on a (0001) Si face yields "apparent macrosteps" with a terrace width of 220 to 280 nm and a step height of 3 to 6 nm. Each macrostep is not a single multiple-height step but composed of a number of "microsteps" with different terrace widths as well as different step heights. Powell et al. [41] also reported macrostep formation on 6H-SiC(0001) Si faces [41]. On a $(000\bar{1})$ C face, the surface is rather flat and no macrosteps are observed. Although 4H-SiC epilayers had basically similar step structures, the 4H-SiC(0001) Si faces exhibited real macrosteps with 110 to 160 nm width and 10 to 15 nm height in some regions.

The mechanism of "apparent macrostep" formation on 6H- and 4H-SiC(0001) Si faces is not clear at present. However, the surface is quite similar to the so-called "hill-and-

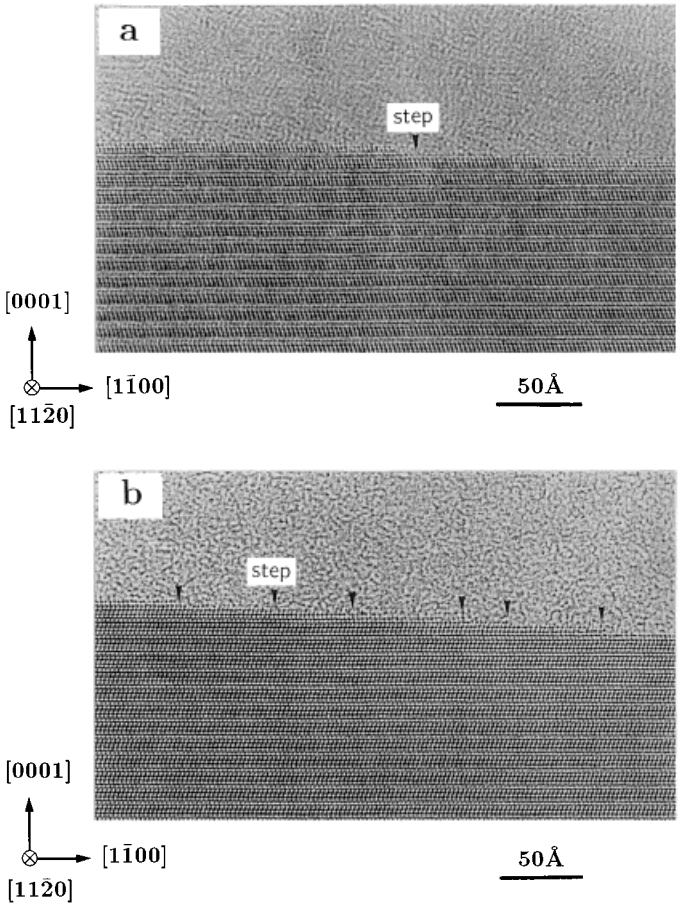

Fig. 8. Typical cross-sectional TEM images for 4H-SiC surfaces grown on a) Si and b) C faces. Substrates are (0001) Si 3.5° off-oriented toward $\langle 11\bar{2}0\rangle$. The samples are examined along the $\langle \bar{1}2\bar{1}0\rangle$ zone axis

valley (or faceted)" structure, which often appears on grown surfaces with off-orientation from a low-index plane [45, 46]. The off-oriented surfaces will spontaneously rearrange to minimize their total surface energies, even if this involves an increase in surface area. The surface free energies of SiC were calculated to be 1767×10^{-7} J/cm^2 for the Si face and 718×10^{-7} J/cm^2 for the C face [47]. Thus, the surface energy may be reduced by the formation of hill-and-valley structure on off-oriented (0001) Si, which has much higher surface energy.

Fig. 8a, b show typical cross-sectional TEM images for 4H-SiC surfaces grown on Si and C faces, respectively, with 3.5° off-angle. The epilayers were produced at a C/Si ratio of 2, and have a thickness of 10 μm. The samples were examined along the $\langle 11\bar{2}0 \rangle$ zone axis to obtain clear lattice images. No island growth on the {0001} terraces are observed, indicating step-flow growth. On a Si face (Fig. 8a), the number of Si–C bilayer at bunched steps is four. It should be noted that the bunched steps correspond to exactly the unit cell of 4H-SiC: ABCB steps in the ABC notation. On a C face (Fig. 8b), however, single bilayer-height steps dominate, and bunched steps are relatively few.

The authors examined more than 200 steps from at least two samples for each condition, and made histograms of step height and terrace width. Fig. 9 and 10 show the histograms of step height for the surfaces of 6H-SiC and 4H-SiC epilayers, respectively. On a 6H-SiC Si face, 88% of steps are composed of three Si–C bilayers (half unit cell), and 7% of steps have six Si–C bilayer height (unit cell). In contrast, single Si–C bilayer-height steps are dominant on C faces, showing a probability of 68%. On the other hand, four-bilayer-height (unit cell) steps are the most dominant (66%) and two-bilayer-height steps show the second highest probability (19%) on a 4H-SiC Si face. On a 4H-SiC C face, however, most (80%) steps have single Si–C bilayer height. It is also noteworthy that even on C faces, small amount of bunched steps have, again, three- or six-bilayer-height in 6H-SiC, and two- or four-bilayer-height in 4H-SiC. The origin of this striking polarity dependence is not known. The migrating species, surface coverage, and exact bond configuration at step edges should be analyzed to reveal the mechanism.

As shown in Figs. 9 and 10, the formation of half-unit-cell or unit-cell height steps seems to be inherent in α-SiC growth. Similar observation has been reported on 6H-SiC

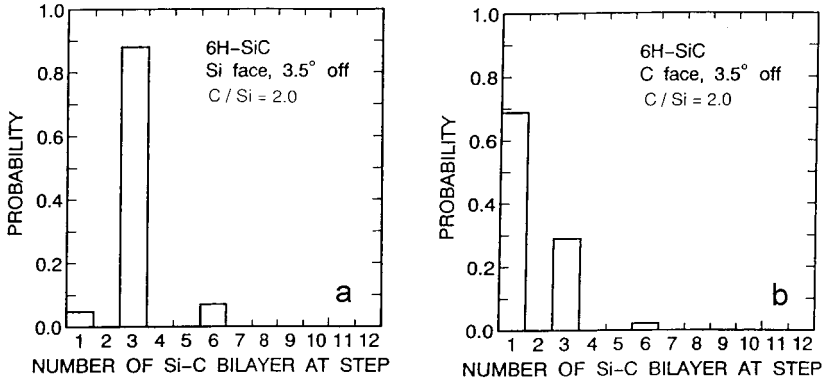

Fig. 9. Histograms of step height for surfaces of 6H-SiC epilayers grown on a) Si and b) C faces. The substrate off-angle is 3.5° toward $\langle 11\bar{2}0 \rangle$. The epilayers were produced with a C/Si ratio of 2

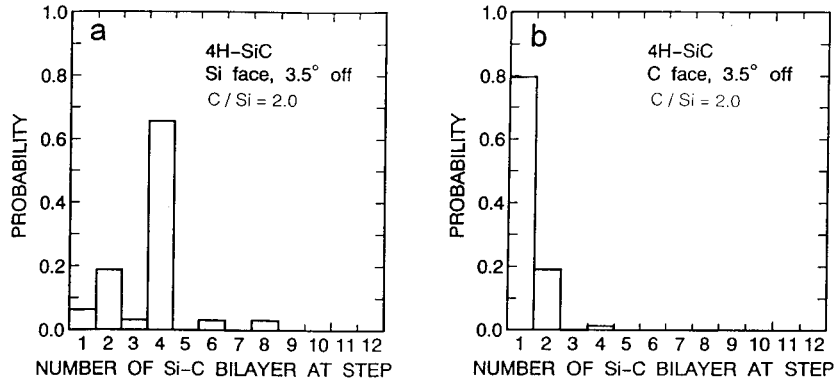

Fig. 10. Histograms of step height for surfaces of 4H-SiC epilayers grown on a) Si and b) C faces. The substrate off-angle is 3.5° toward $\langle 11\bar{2}0 \rangle$. The epilayers were produced with a C/Si ratio of 2

surfaces grown by the Lely method [48] and MBE [49]. Thus, the origin of step bunching in SiC may be correlated with the surface equilibrium process. Heine et al. [18] suggested that surface energies are different for each SiC bilayer plane owing to the peculiar stacking sequence. Different surface energy may lead to different step velocity among different Si–C bilayers, and thereby causes "structurally-induced macrostep formation", of which details will be discussed elsewhere [50].

On a Si face with 3.5° off-angle, the average terrace widths experimentally obtained were 12.4 nm for 6H-SiC and 16.8 nm for 4H-SiC. The different average terrace width between 6H-SiC and 4H-SiC, in spite of the identical off-angle, originates from the different height of multiple steps as described above. From a viewpoint of epitaxial growth, narrow terraces are preferable to achieve step-flow growth. This is crucial in SiC growth, because supersaturation increases on larger terraces, leading to 3C-SiC nucleation. In this sense, 4H-SiC, which shows larger terrace widths, may have the disadvantage of relatively higher probability for nucleation on terraces. To overcome this problem, a slightly higher growth temperature would be helpful, since the longer surface diffusion length of adsorbed species and lower supersaturation on terraces are expected at higher temperatures. Larger off-angles of substrates might be also effective in 4H-SiC growth [51]. On the other hand, C faces showed much smaller average terrace widths (4 to 5 nm), owing to fewer bunched steps. This might be one reason why epilayers grown on C faces exhibit a very flat surface even for 4H-SiC.

4. Impurity Doping and Characterization

4.1 Characterization of unintentionally doped n-type epilayers

For SiC epilayers grown under optimum condition, very smooth surfaces can be obtained on both Si and C faces (especially on a C face), and almost all the surface pits originate from so-called "micropipes" in the substrates, except for 4H-SiC epilayers on a Si face, on which a small density of triangular pits is still existing even on 8° off-oriented substrates. Although it is difficult to detect small micropipes on as-polished surfaces (before growth), triangular pits are formed at the micropipe positions after epitaxial growth. These pits are accompanied with "shadows" due to the impedance of step-advance.

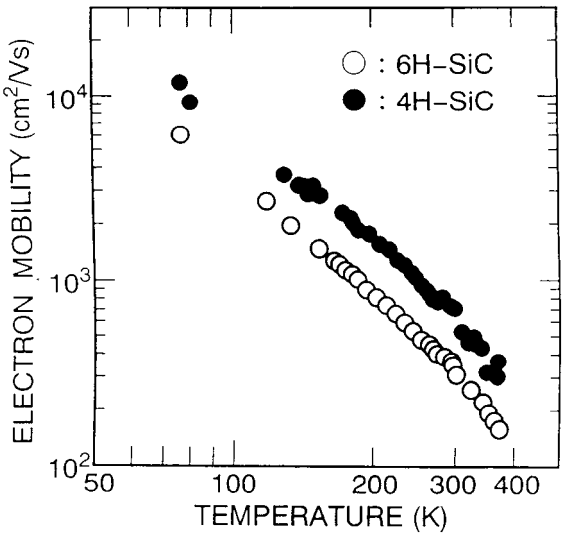

Fig. 11. Temperature dependence of electron mobility of 6H- and 4H-SiC epilayers with a net donor concentration of 4×10^{16} cm^{-3}

In photoluminescence (PL) measurements at 2 to 15 K, PL spectra are governed by the lines due to the recombination of an exciton bound to neutral nitrogen and free excitons. The N donor–Al acceptor pair band is very weak, whereas the donor–acceptor pair luminescence is dominant in substrates. PL spectra indicated very little contamination of Al acceptor, which would normally show the Al bound exciton peaks [52].

Fig. 11 shows the temperature dependence of electron mobility of 6H- and 4H-SiC with a net donor concentration of 4×10^{16} cm^{-3}. The mobility is 351 cm^2/Vs for 6H-SiC and 724 cm^2/Vs for 4H-SiC at room temperature [21]. The mobility increases with lowering temperature, and reaches up to 6050 cm^2/Vs for 6H-SiC and 11000 cm^2/Vs for 4H-SiC at 77 K. The increasing mobility at low temperature reflects the low impurity compensation in the epilayers.

Isothermal capacitance transient spectroscopy (ICTS) measurements on Schottky structures of n-type 6H-SiC epilayers have shown very small concentrations (below the detection limit) of deep traps [53]. Recently, the authors' group succeeded to reveal deep electron traps in both 6H- and 4H-SiC epilayers by high-resolution deep level transient spectroscopy (DLTS). The samples used in this study were 8 to 10 μm thick epilayers with a net donor concentration of 2×10^{15} to 1×10^{16} cm^{-3}. Fig. 12a, b show the DLTS

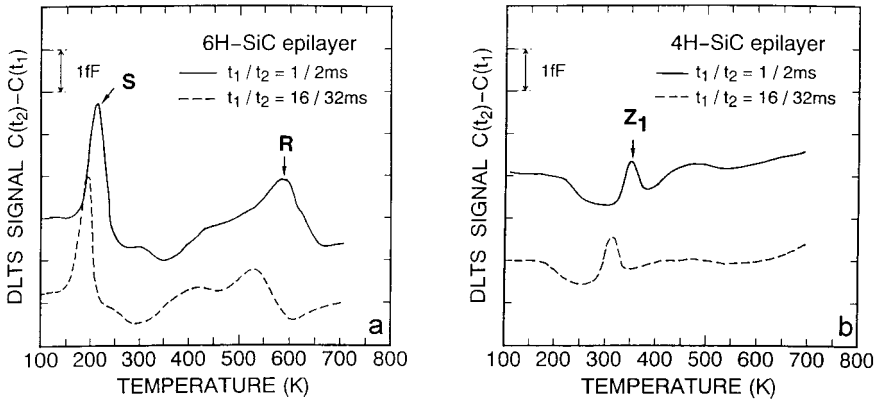

Fig. 12. DLTS spectra obtained from as-grown a) 6H-SiC and b) 4H-SiC epilayers with a net donor concentration of 2×10^{15} cm^{-3}

spectra obtained from as-grown 6H-SiC and 4H-SiC epilayers, respectively. The spectra of 6H-SiC exhibit two peaks both at concentrations of 4×10^{12} cm^{-3}. An Arrhenius plot evaluation of these two peaks revealed the activation energies of 0.39 to 0.43 and 1.17 to 1.27 eV with respect to the conduction band, respectively. These peaks are termed S and R, based on a previous report [55]. On the other hand, only one peak is observed in 4H-SiC epilayers. The trap concentration and activation energy are estimated to be 4×10^{12} cm^{-3} and 0.63 to 0.68 eV, respectively. This trap can be attributed to the Z_1-center, an acceptor-like complex containing intrinsic defects [56]. Thus, both 6H- and 4H-SiC epilayers have low concentration of deep levels, indicating high quality sufficient for device applications.

4.2 In-situ doping of impurities

In-situ n-type doping can easily be achieved by the introduction of N_2 during epitaxial growth. The donor concentration estimated from capacitance–voltage (C–V) characteristics was proportional to the N_2 flow rate in the wide range on both Si and C faces, in agreement with the results by Wang et al. [57] and Karmann et al. [9], though these previous studies employed only 6H-SiC(0001) Si substrates.

Recently, Larkin et al. [58] have found that the doping efficiency of impurities strongly depends on the C/Si ratio (or Si/C ratio) during CVD growth (site-competition epitaxy). The growth under a higher C/Si ratio leads to the lower N concentration in the epilayers. This phenomenon can be explained by the fact that the higher C atom coverage on a growing surface prevents the incorporation of N atoms, which substitute at the C site, into crystals. Fig. 13 shows our result on the C/Si ratio dependence of background doping level of unintentionally doped 4H-SiC epilayers. In the case of C/Si ratio of 2, no significant difference was observed between epilayers on Si and C faces. On a Si face, the donor concentration can drastically be reduced by increasing the C/Si ratio. The lowest value in our system is in the range of 5×10^{13} to 1×10^{14} cm^{-3}. On a C face, however, the donor concentration is not sensitive to the C/Si ratio. We observed a similar C/Si ratio dependence in intentional N doping [59]. On the other hand, the incorporation of aluminum (Al) and boron (B) atoms, which substitute at the Si site, is enhanced under C-rich conditions on a Si face.

Fig. 14 shows the electron mobility at room temperature in the basal plane versus carrier concentration of

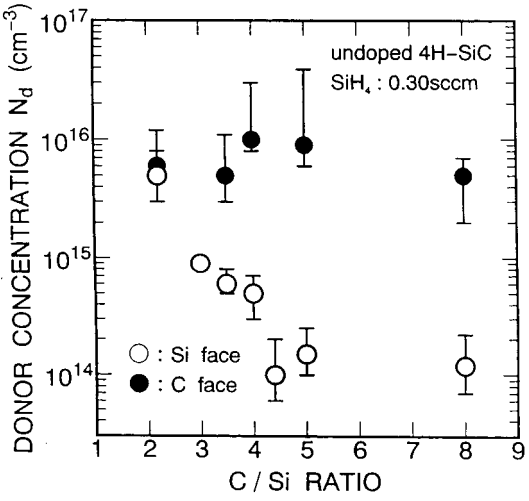

Fig. 13. C/Si ratio dependence of donor concentration for unintentionally doped 4H-SiC epilayers

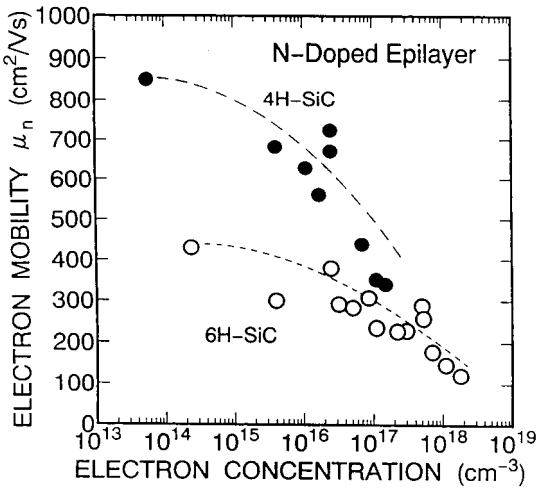

Fig. 14. Electron mobility vs. carrier concentration of n-type 6H- and 4H-SiC epilayers at room temperature

6H- and 4H-SiC epilayers. As is well-known, 4H-SiC exhibits a two times higher electron mobility than 6H-SiC. However, the difference seems to be small for heavily doped layers, in agreement with a previous report [60]. As shown in Fig. 13, very low-doped epilayers can be produced on Si faces by growing under C-rich conditions. For very low-doped epilayers, which were produced with a C/Si ratio of 4 to 5, high electron mobilities of 431 cm^2/Vs ($n = 2 \times 10^{14}$ cm^{-3}) for 6H-SiC and 851 cm^2/Vs ($n = 6 \times 10^{13}$ cm^{-3}) for 4H-SiC were obtained at room temperature. For device applications, 4H-SiC is much more attractive owing to its higher electron mobility and smaller anisotropy [60, 61].

The addition of a small amount of TMA is effective for in-situ p-type doping. Although most Al-doped epilayers showed very smooth surfaces, surface pits and hillocks were observed in heavily doped (Al concentration $>3 \times 10^{18}$ cm^{-3}) samples grown on C faces. The supply of TMA causes the shift of growth conditions toward C-rich ambience due to the release of CH_3 species from TMA molecules. The surface migration is suppressed and the nucleation is promoted under C-rich growth conditions [62]. Besides, C faces easily suffer from two-dimensional nucleation, due to its low critical supersaturation ratio [35, 40]. This may be the reason for the surface roughening of heavily Al-doped epilayers grown on C faces. The Al acceptor concentration versus TMA flow rate is shown in Fig. 15. The flow rates of SiH_4 and C_3H_8 are 0.30 and 0.20 sccm (C/Si ratio = 2.0), respectively. The acceptor concentration estimated from C–V measurements agreed well with the Al concentration determined by secondary ion mass spectro-

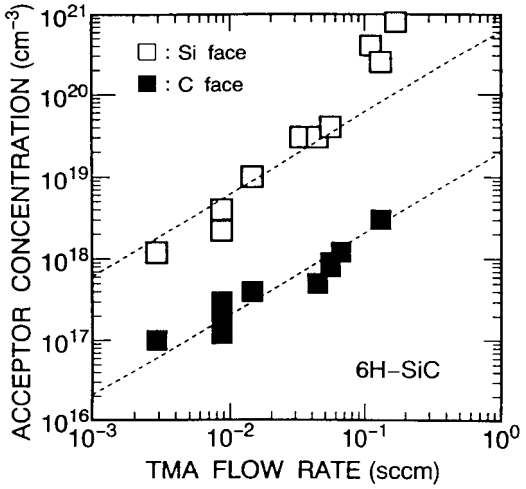

Fig. 15. Al acceptor concentration vs. TMA flow rate in epitaxial growth of 6H-SiC. The growth was performed at 1500 °C with a C/Si ratio of 2

scopy (SIMS) measurements. The doping efficiency is much higher on Si faces than on C faces by a factor of 10 to 80. On a Si face, the acceptor concentration increases superlinearly with the TMA supply. This superlinearity may be caused by the increased effective C/Si ratio under high TMA flow conditions, enhancing the Al incorporation, mentioned above. It should be noted that heavily doped p-type layers can be grown only on a Si face.

Because of the high ionization energy Al acceptors (242 meV in 6H-SiC) [63], the activation ratio p/N_a (p hole concentration, N_a acceptor concentration) was as low as 0.01 to 0.1 at room temperature. However, a very high hole concentration of 4 to $6 \times 10^{19}\,\mathrm{cm}^{-3}$ could be achieved for heavily doped epilayers (Al concentration is in the mid $10^{20}\,\mathrm{cm}^{-3}$ range). This result might arise from the decreased ionization energy in heavily doped samples, or from the formation of impurity band caused by the impurity–impurity interaction [64]. The lowest p-type resistivity was $0.042\,\Omega$ cm for 6H-SiC and $0.025\,\Omega$ cm for 4H-SiC, which were obtained on Si faces. These p^+ epilayers can be successfully used for contact layers to reduce contact resistances. Thus, each surface (Si, C face) possesses its inherent properties, and the substrate polarity should be selected, depending on the device structure, to achieve the full potential of SiC [65].

5. Summary

Step-controlled epitaxial growth of SiC on off-oriented SiC{0001} substrates was reviewed. Step-flow growth is essential to realize polytype replication in epilayers without 3C-SiC inclusions through two-dimensional nucleation on terraces. The introduction of a substrate off-angle induces the change of rate-determining step from surface-reaction control to diffusion control. Critical growth conditions where growth mode changes from step-flow to two-dimensional nucleation were predicted as a function of growth temperature, growth rate, and substrate off-angle, by using a model describing SiC growth on vicinal SiC{0001}. Step structures of epilayer surfaces depended on the substrate polarity as well as polytypes. Dominant step heights corresponded to the half or full unit cell of SiC polytypes.

The background doping level of epilayers could be reduced to less than $1 \times 10^{14}\,\mathrm{cm}^{-3}$ by the growth under C-rich conditions, by which very high electron mobilities of $431\,\mathrm{cm}^2/\mathrm{Vs}$ for 6H-SiC and $851\,\mathrm{cm}^2/\mathrm{Vs}$ for 4H-SiC were obtained. Deep level analyses revealed that the trap concentration was in the $10^{12}\,\mathrm{cm}^{-3}$ range, indicating very high quality of the epilayers. Excellent doping control has been obtained by in-situ doping of a nitrogen donor and an aluminum acceptor.

Acknowledgements The authors wish to express their gratitude to Prof. W. J. Choyke of University of Pittsburgh, Dr. G. Pensl and Mr. T. Dalibor of University of Erlangen-Nürnberg for collaborative works on characterization of epilayers. They also would like to thank Prof. T. Ohachi of Doshisha University for the use of RHEED equipment, and Mr. T. Nakata of Ion Engineering Research Institute and Mr. T. Okano of Matsushita Technoresearch, Inc. for TEM analyses.

References

[1] M. Bhatnagar and B. J. Baliga, IEEE Trans. Electron Devices **40**, 645 (1993).
[2] V. J. Jennings, A. Sommer, and H. Chang, J. Electrochem. Soc. **113**, 728 (1966).
[3] W. von Muench and I. Phaffeneder, Thin Solid Films **31**, 39 (1976).

[4] S. Yoshida, E. Sakuma, H. Okumura, S. Misawa, and K. Endo, J. Appl. Phys. **62**, 303 (1987).
[5] N. Kuroda, K. Shibahara, W. S. Yoo, S. Nishino, and H. Matsunami, Extended Abstracts 34th Spring Meeting of the Japan Society of Applied Physics and Related Societies, Tokyo, 1987 (p. 135) (in Japanese).
[6] N. Kuroda, K. Shibahara, W. S. Yoo, S. Nishino, and H. Matsunami, Extended Abstracts 19th Conf. Solid State Devices and Materials, Tokyo, 1987 (p. 227).
[7] H. S. Kong, J. T. Glass, and R. F. Davis, J. Appl. Phys. **64**, 2672 (1988).
[8] J. A. Powell, D. J. Larkin, L. G. Matus, W. J. Choyke, J. L. Bradshaw, L. Henderson, M. Yoganathan, J. Yang, and P. Pirouz, Appl. Phys. Lett. **56**, 1442 (1990).
[9] S. Karmann, W. Suttrop, A. Schöner, M. Schadt, C. Haberstroh, F. Engelbrecht, R. Helbig, and G. Pensl, J. Appl. Phys. **72**, 5437 (1992).
[10] O. Kordina, A. Henry, C. Hallin, R. C. Glass, A. O. Konstantinov, C. Hemmingsson, N. T. Son, and E. Janzén, Mater. Res. Soc. Symp. Proc. **339**, 405 (1994).
[11] A. A. Burk, Jr., D. L. Barrett, H. M. Hobgood, R. R. Siergiej, T. T. Braggins, R. C. Clarke, G. W. Eldridge, C. D. Brandt, D. J. Larkin, J. A. Powell, and W. J. Choyke, Silicon Carbide and Related Materials, Eds. M. G. Spencer, R. P. Devaty, J. A. Edmond, M. A. Khan, R. Kaplan, and M. M. Rahman, Institute of Physics, Bristol, 1994 (p. 29).
[12] R. Rupp, P. Lanig, J. Volkel, and D. Stephani, J. Cryst. Growth **146**, 37 (1995).
[13] N. Nordell, S. G. Andersson, and A. Schöner, Silicon Carbide and Related Materials, 1995, Eds. S. Nakashima, H. Matsunami, S. Yoshida, H. Harima, Institute of Physics, Bristol, 1996 (p. 81).
[14] S. Nakashima, H. Matsunami, S. Yoshida, H. Harima (Eds.), Silicon Carbide and Related Materials, 1995, Institute of Physics, Bristol, 1996 (Chapter 4).
[15] W. von Muench and I. Pfaffeneder, J. Electrochem. Soc. **122**, 642 (1975).
[16] A. Suzuki, H. Ashida, N. Furui, K. Mameno, and H. Matsunami, Jpn. J. Appl. Phys. **21**, 579 (1982).
[17] H. Matsunami, T. Ueda, and H. Nishino, Mater. Res. Soc. Symp. Proc. **162**, 397 (1990).
[18] V. Heine, C. Cheng, and R. J. Needs, J. Amer. Ceram. Soc. **74**, 2630 (1991).
[19] W. S. Yoo and H. Matsunami, Amorphous and Crystalline Silicon Carbide IV, Eds. C. Y. Yang, M. M. Rahman, and G. L. Harris, Springer-Verlag, Berlin 1992 (p. 66).
[20] A. R. Verma and P. Krishna (Eds.), Polymorphism and Polytypism in Crystals, John Wiley & Sons, Inc., New York 1966.
[21] A. Itoh, H. Akita, T. Kimoto, and H. Matsunami, Appl. Phys. Lett. **65**, 1400 (1994).
[22] T. Kimoto, Doctoral Thesis, Kyoto University, 1995.
[23] Yu. M. Tairov, V. F. Tsvetkov, S. K. Lilov, and G. K. Safaraliev, J. Cryst. Growth **36**, 147 (1976).
[24] J. A. Powell, J. B. Petit, J. H. Edgar, I. G. Jenkins, L. G. Matus, J. W. Yang, P. Pirouz, W. J. Choyke, L. Clemen, and M. Yoganathan, Appl. Phys. Lett. **59**, 333 (1991).
[25] C. Hallin, A. O. Konstantinov, O. Kordina, and E. Janzén, see [13] (p. 85).
[26] Y. Matsushita, T. Nakata, T. Uetani, T. Yamaguchi, and T. Niina, Jpn. J. Appl. Phys. **29**, L343 (1990).
[27] T. Ueda, H. Nishino, and H. Matsunami, J. Cryst. Growth **104**, 695 (1990).
[28] S. Karmann, C. Haberstroh, F. Engelbrecht, W. Suttrop, A. Schöner, M. Schadt, R. Helbig, G. Pensl, R. A. Stein, and S. Leibenzeder, Physica **185B**, 75 (1993).
[29] M. D. Allendorf and R. J. Kee, J. Electrochem. Soc. **138**, 841 (1991).
[30] C. D. Stinespring and J. C. Wohmhoudt, J. Cryst. Growth **87**, 481 (1988).
[31] A. O. Konstantinov, C. Hallin, O. Kordina, and E. Janzén, J. Appl. Phys. **80**, 5704 (1996).
[32] A. A. Burk, Jr. and L. B. Rowland, J. Cryst. Growth **167**, 586 (1996).
[33] T. Kimoto, H. Nishino, W. S. Yoo, and H. Matsunami, J. Appl. Phys. **73**, 726 (1993).
[34] H. S. Kong, J. T. Glass, and R. F. Davis, J. Mater. Res. **4**, 204 (1989).
[35] T. Kimoto and H. Matsunami, J. Appl. Phys. **76**, 7322 (1994).
[36] H. Matsunami and T. Kimoto, Mater. Res. Soc. Symp. Proc. **339**, 369 (1994).
[37] B. Wessels, H. C. Gatos, and A. F. Witt, Sillicon Carbide, 1973, Eds. R. C. Marshall, J. W. Faust, Jr., and C. E. Ryan, University of South Carolina Press, Columbia, 1974 (p. 25).

[38] F. C. EVERSTEYN, P. J. W. SEVERIN, C. H. J. v. d. BREKEL, and H. L. PEEK, J. Electrochem. Soc. **117**, 925 (1970).
[39] W. K. BURTON, N. CABRERA, and F. C. FRANK, Phil. Trans. Roy. Soc. **A243**, 299 (1951).
[40] T. KIMOTO and H. MATSUNAMI, J. Appl. Phys. **75**, 850 (1994).
[41] J. A. POWELL, D. J. LARKIN, and P. B. ABEL, J. Electronic Mater. **24**, 295 (1995).
[42] T. KIMOTO, A. ITOH, and H. MATSUNAMI, Appl. Phys. Lett. **66**, 3645 (1995).
[43] S. TANAKA, R. C. KERN, R. F. DAVIS, J. F. WENDELKEN, and J. WU, Surf. Sci. **350**, 247 (1996).
[44] J. A. POWELL, D. J. LARKIN, P. B. ABEL, L. ZHOU, and P. PIROUZ, see [13] (p. 77).
[45] C. HERRING, Phys. Rev. **82**, 87 (1951).
[46] W. A. TILLER, The Science of Crystallization: Microscopic Interfacial Phenomena, Chap. 2, Cambridge University Press, Cambridge 1991.
[47] T. TAKAI, T. HALICIOGLU, and W. A. TILLER, Surf. Sci. **164**, 341 (1985).
[48] S. TYC, see [11] (p. 333).
[49] S. TANAKA, R. S. KERN, and R. F. DAVIS, Appl. Phys. Lett. **65**, 2851 (1994).
[50] T. KIMOTO, A. ITOH, H. MATSUNAMI, and T. OKANO, J. Appl. Phys. **81**, 3494 (1997).
[51] V. F. TSVETKOV, S. T. ALLEN, H. S. KONG, and C. H. CARTER, JR., see [13] (p. 17).
[52] L. L. CLEMEN, R. P. DEVATY, M. F. MACMILLAN, M. YOGANATHAN, W. J. CHOYKE, D. J. LARKIN, J. A. POWELL, J. A. EDMOND, and H. S. KONG, Appl. Phys. Lett. **62**, 2953 (1993).
[53] S. JANG, T. KIMOTO, and H. MATSUNAMI, Appl. Phys. Lett. **65**, 581 (1994).
[54] T. DALIBOR, G. PENSL, T. KIMOTO, H. MATSUNAMI, S. SRIDHARA, R. P. DEVATY, and W. J. CHOYKE, presented at the 1st Europ. Conf. Silicon Carbide and Related Materials, Crete, 1996.
[55] M. M. ANIKIN, A. N. ANDREEV, A. A. LEBEDEV, S. N. PYATKO, M. G. RASTEGAEVA, N. S. SAVKINA, A. M. STREL'CHUK, A. L. SYRKIN, and V. E. CHELNOKOV, Soviet Phys. – Semicond. **25**, 198 (1991).
[56] T. DALIBOR, C. PEPPERMÜLLER, G. PENSL, S. SRIDHARA, R. P. DEVATY, W. J. CHOYKE, A. ITOH, T. KIMOTO, and H. MATSUNAMI, see [13] (p. 517).
[57] Y. C. WANG, R. F. DAVIS, and J. A. EDMOND, J. Electronic Mater. **20**, 289 (1991).
[58] D. J. LARKIN, P. G. NEUDECK, J. A. POWELL, and L. G. MATUS, Appl. Phys. Lett. **65**, 1659 (1994).
[59] T. KIMOTO, A. ITOH, and H. MATSUNAMI, Appl. Phys. Lett. **67**, 2385 (1995).
[60] 85 (1995).
[61] W. J. SCHAFFER, G. H. NEGLEY, K. G. IRVINE, and J. W. PALMOUR, Mater. Res. Soc. Symp. Proc. **339**, 595 (1994).
[62] M. SCHADT, G. PENSL, R. P. DEVATY, W. J. CHOYKE, R. STEIN, and D. STEPHANI, Appl. Phys. Lett. **65**, 3120 (1994).
[63] T. KIMOTO and H. MATSUNAMI, J. Appl. Phys. **78**, 3132 (1995).
[64] A. SCHÖNER, N. NORDELL, K. ROTTNER, R. HELBIG, and G. PENSL, see [13] (p. 493).
[65] V. I. FISTUL, Heavily Doped Semiconductors, Plenum Press, New York 1969.
[66] T. KIMOTO, A. ITOH, O. TAKEMURA, S. KOBAYASHI, and H. MATSUNAMI, Extended Abstracts 38th Electron. Mater. Conf., Santa Barbara, 1996 (p. 19).